Tensor DoA estimation with directional elements

Francesca Raimondi, Elisabeth Delevoye, Pierre Comon

Tensor DoA estimation with directional elements

Francesca Raimondi[13], Elisabeth Delevoye[23], and Pierre Comon[13]

[1] GIPSA-Lab, CNRS,
[2] Univ. Grenoble Alpes, F-38000 Grenoble, France
[3] CEA, Leti, Minatec Campus, 17 rue des Martyrs - 38054 Grenoble Cedex 9, France

Abstract. This paper introduces directivity gain pattern as a physical diversity for tensor array processing, in addition to time and space shift diversities. We show that tensor formulation allows to estimate Directions of Arrival (DoAs) under the assumption of unknown gain pattern, improving the performance of the omnidirectional case. The proposed approach is then applied to biologically inspired acoustic elements.

Keywords: DoA estimation, Directivity, Gain, Patterns, Smart Antennas, Directional Arrays

1 Introduction

Directional sensor arrays have been adressed in the context of smart antennas, through beamforming techniques [1] and null-steering (see [2, 3] for a list of examples). However, very few studies have investigated directional elements for Direction of Arrival (DoA) estimation, such as [4, 5], both with Uniform Circular Arrays (UCA). High resolution DoA estimation with known sensor gains through the MUSIC [6] algorithm has been further studied in [3], where the effects and advantages of different directivity patterns have been considered, as well as a realistic dipole array implementation; a derivation of Cramér-Rao Bound (CRB) for directional elements of a UCA is also included.

If sensors are omnidirectional (as in most literature in array processing), only relative phase differences between sensors are needed to extract DoA information. However, if the antenna elements are directional, one must jointly exploit gain and phase differences in every direction of interest. To our knowledge, existing studies of DoA estimation in the presence of directional elements only cover the case of known directivity gains: our aim is to treat the case of DoA estimation for sensors with *unknown* gain patterns.

Tensor analysis has been extended to DoA estimation, requiring at least three physical diversities, such as time, space and space shift [7, 8]. Recently, a general formulation for tensor array processing has been extended to the wideband case through multiple physical diversities in [9]. The possibility of the inclusion of directivity gains into the formulation was suggested therein, but not further investigated.

This work was supported by the ERC Grant AdG-2013-320594 "Decoda".

Our paper introduces the directivity gain pattern in the tensor model for array processing, thus allowing to exploit directional elements even when their directivity gains are not known. Computer results are reported as a function of SNR and sensor directivity, in comparison to Cramér-Rao Bounds (CRB). The effect of directivity patterns is also shown with respect to the omnidirectional case. Finally we show the practical interest of the proposed methods through the analysis of a small network of microsensors, bio-inspired from insects [10, 11].

2 Physical Model

2.1 Multiple Source Multiple Sensor Framework in the Far-Field

Assume R source signals impinge on an array of L sensors, each located at a position in space defined by a vector $\boldsymbol{p}_\ell \in \mathbb{R}^3$. For each source, denote the angles of arrival by a vector $\boldsymbol{\theta}_r = [\phi_r, \psi_r]$ in 3D, $1 \leq r \leq R$, or by a scalar $\theta_r = \phi_r$ if we restrict our attention to a localization problem in 2D.

We assume that the signal received at the ℓth sensor at time t follows the additive model below:

$$x_\ell[t] = \sum_{r=1}^{R} g_\ell(\boldsymbol{\theta}_r)\, \varsigma_r[t - \tau_\ell(\boldsymbol{\theta}_r)] + n_\ell[t], \quad 1 \leq \ell \leq L \tag{1}$$

where $\varsigma_r[t] \in \mathbb{R}$ is the rth source signal, τ_ℓ is the delay of arrival and $n_\ell[t]$ refers to noise. If c denotes the (constant) propagation speed, we have $\tau_\ell(\boldsymbol{\theta}) = \boldsymbol{p}_\ell^{\mathsf{T}} \boldsymbol{d}(\boldsymbol{\theta})/c$, where $\boldsymbol{d}(\boldsymbol{\theta})$ is the unit modulus vector pointing in direction $\boldsymbol{\theta}$.

Notice that in our framework, each sensor may have its own gain pattern $g_\ell : \mathbb{R} \longmapsto \mathbb{R}^+$. If the signal is narrowband around radial frequency ω_0, we can work in baseband and write the complex envelope of received signals as

$$x_\ell(t) = \sum_{r=1}^{R} g_\ell(\boldsymbol{\theta}_r)\, s_r(t)\, e^{\imath\omega_0 \tau_\ell(\boldsymbol{\theta}_r)} + n_\ell(t) \tag{2}$$

where $s_r(t)$ is the complex envelope of the rth waveform $\varsigma_r(t)$ around ω_0. Now, defining $\boldsymbol{x}(t) = [x_1(t), \ldots, x_L(t)]^T$ leads to the standard compact writing [6]:

$$\boldsymbol{x}(t) = \boldsymbol{A}(\boldsymbol{\theta})\, \boldsymbol{s}(t) + \boldsymbol{n}(t) \in \mathbb{C}^{L \times 1} \tag{3}$$

where $\boldsymbol{s}(t) = [s_1(t), \ldots, s_R(t)]^T$ and $\boldsymbol{n}(t) = [n_1(t), \ldots, n_L(t)]^T$. The $L \times R$ steering matrix $\boldsymbol{A} = [\boldsymbol{a}(\boldsymbol{\theta}_1), \ldots, \boldsymbol{a}(\boldsymbol{\theta}_R)]$ has elements $A_{\ell r} = a_\ell(\boldsymbol{\theta}_r) = g_\ell(\boldsymbol{\theta}_r)\, e^{\imath\omega_0 \tau_\ell(\boldsymbol{\theta}_r)}$.

2.2 Multiple Sub-Arrays

Now, following the original idea developed in [7], assume we have at our disposal a set of M sub-arrays, each containing L sensors, and deducible from each other by a translation. Choose one of these sub-arrays as a reference, label it with $m = 1$, and denote by $\boldsymbol{\delta}_m$, $m > 1$ the vector defining the translation to obtain

the $M-1$ remaining sub-arrays. To simplify subsequent equations, we also define $\boldsymbol{\delta}_1 = \mathbf{0}$. The delay of arrival of the rth source to reach sensor ℓ of array m is then $\tau_\ell(\boldsymbol{\theta}_r) + \zeta_m(\boldsymbol{\theta}_r)$ where $\zeta_m(\boldsymbol{\theta}_r) = \boldsymbol{\delta}_m^\mathsf{T}\boldsymbol{d}(\boldsymbol{\theta}_r)/c$. Then, at fixed radial frequency ω_0, the complex envelope of the signal received at the ℓth sensor of the mth sub-array can be written as $\mathcal{X}_{\ell mt} = \mathcal{M}_{\ell mt} + \mathcal{N}_{\ell mt}$, where [9]:

$$\begin{aligned} \mathcal{M}_{\ell mt} &= \sum_{r=1}^{R} A_{\ell r}\, B_{mr}\, S_{rt} \in \mathbb{C}^{L\times M\times T} \\ \text{with} \quad & \begin{cases} A_{\ell r} &= g_\ell(\boldsymbol{\theta}_r)\, e^{-\jmath\omega_0\tau_\ell(\boldsymbol{\theta}_r)} \\ B_{mr} &= e^{-\jmath\omega_0\zeta_m(\boldsymbol{\theta}_r)} \\ S_{rt} &= s_r(t) \end{cases} \end{aligned} \tag{4}$$

Notice that $L \times R$ steering and pattern matrix $\boldsymbol{A}$ is the same as in Section 2.1. Space shift elements of $M \times R$ steering matrix $\boldsymbol{B}$ are a function of the delay of arrival on each sub-array m. Finally, source complex envelopes constitute $T \times R$ matrix $\boldsymbol{S}$. We shall work under the assumptions summarized below.

Assumptions

1. The first sensor ($\ell = 1$) is taken as origin, so that $\boldsymbol{p}_1 = \mathbf{0}$, and has a unit gain in all directions, *i.e.* $g_1(\theta) = 1$, $\forall\theta$.
2. The first sub-array is considered as a reference, so that $\boldsymbol{\delta}_1 = \mathbf{0}$.
3. The space shifts $\boldsymbol{\delta}_1, \ldots, \boldsymbol{\delta}_M$ are known, whereas sensor positions $\boldsymbol{p}_\ell$, $\ell \neq 1$ and gains $g_\ell(\theta)$, $\ell \neq 1$ are unknown.
4. The sensor gains $g_\ell(\theta)$ are real (which is actually equivalent to assuming that their phase is known) and frequency-flat.
5. Sources $s_r(t)$ are deterministic.
6. The wave propagation speed c does not depend on frequency (*i.e.* the medium is not dispersive).
7. Noise is circular complex white Gaussian.

Notice that Assumptions 1 and 2 are not restrictive, and permit to fix the scale indeterminacies in model (4), as pointed out in the next section. Assumption 4 means that L continuous real functions are unknown. However, they need to be known only at values θ_r, so that we may consider only $g_{\ell r} = g_\ell(\theta_r)$ as unknowns. The circularity could be relaxed in Assumption 7 to the price of an increased notational complexity, as in [8].

If sensors within a sub-array overlap, $\boldsymbol{p}_\ell = 0\,\forall\ell$ and matrix $\boldsymbol{A}$ only contains information about directivity gains: $A_{\ell r} = g_\ell(\boldsymbol{\theta}_r)$. Therefore, the only space information is carried by space-shift matrix $\boldsymbol{B}$. On the other hand, if sensors within a sub-array do not overlap, $\boldsymbol{p}_\ell = 0 \iff \ell = 1$.

2.3 Tensor Decomposition

Any tensor represented by an array $\boldsymbol{\mathcal{M}}$ of size $L \times M \times T$ can be decomposed into a sum of R decomposable terms: $\boldsymbol{\mathcal{M}} = \sum_{r=1}^{R} \boldsymbol{\mathcal{D}}(r)$. By *decomposable*, it is meant that there exist R triplets of vectors $(\boldsymbol{u}(r), \boldsymbol{v}(r), \boldsymbol{w}(r))$

such that $\boldsymbol{\mathcal{D}}_{\ell mt}(r) = u_\ell(r)v_m(r)w_t(r)$. When R is minimal, it is called tensor rank, and this decomposition is unique if R is not too large; for instance, $R \leq (L-1)(M-1) \leq T-2$ is sufficient almost surely [12].

Hence in the absence of noise, one can identify every term in (4) with a decomposable tensor, that is: $A_{\ell r}B_{mr}S_{rt} = u_\ell(r)\, v_m(r)\, w_t(r)$. This identifiability property is the main motivation in resorting to tensor-based algorithms. However, there is still a *scaling ambiguity* that cannot be resolved, in general. In fact, denote by $\boldsymbol{a}_r$, $\boldsymbol{b}_r$ and $\boldsymbol{s}_r$ the columns of matrices $\boldsymbol{A}$, $\boldsymbol{B}$ and $\boldsymbol{S}$, respectively. Even if the entries $\boldsymbol{\mathcal{D}}_{\ell mt}(r) = A_{\ell r}B_{mr}S_{rt}$ are known, which we shall denote as $\boldsymbol{\mathcal{D}}(r) = \boldsymbol{a}_r \otimes \boldsymbol{b}_r \otimes \boldsymbol{s}_r$, column vectors are only determined up to scaling factors since $\boldsymbol{a}_r \otimes \boldsymbol{b}_r \otimes \boldsymbol{s}_r = \alpha\boldsymbol{a}_r \otimes \beta\boldsymbol{b}_r \otimes \frac{1}{\alpha\beta}\boldsymbol{s}_r$, for any pair of nonzero scalars (α, β). In other words, this leaves $2R$ scalar unknowns, unless some other constraints are available. In the present context, we precisely know that the first entry of $\boldsymbol{a}_r$ and $\boldsymbol{b}_r$ are equal to 1, $\forall r$, because of Assumptions 1 and 2. These constraints hence completely fix scaling indeterminacies.

2.4 Acquisition System and Directivity Gains

For the sake of simplicity, we consider sources that are coplanar with the acquisition system: sensor positions become $\boldsymbol{p}_\ell = [p_\ell^x, p_\ell^y]$, and $\tau_\ell(\boldsymbol{\theta})$ becomes $\tau_\ell(\theta_r) = p_\ell^x \cos(\theta_r) + p_\ell^y \sin(\theta_r)$, both functions of azimuth only. This amounts to considering elevation $\psi_r = \pi/2$, $\forall r$. We choose to work with a UCA of radius ρ, with $p_\ell^x = \rho\cos(2\pi\ell/L)$ and $p_\ell^x = \rho\sin(2\pi\ell/L)$ [3].

Without loss of generality, we assume that all the sensors within a sub-array have identical directivity pattern $g(\cdot)$, with maximum gain in the radial direction from the center of the array: $g_\ell(\theta_r) = g(\theta_r - 2\pi\ell/L)$. Function $g(\theta) = \sqrt{G(\theta)}$ is chosen to be a simple nonnegative, smooth and 2π-periodical function, with

$$G_\gamma(\theta) = \frac{D(\gamma)}{2^\gamma}\,(1+\cos(\theta))^\gamma \tag{5}$$

and parameter γ controls the directivity $D(\gamma) = \frac{2^\gamma 2\pi}{\int_0^{2\pi}(1+\cos(\theta))^\gamma d\theta}$.

3 Identifiability of Sources and DoA

The tensor model in (4) can be expressed in vector form as

$$\boldsymbol{x} = \sum_{r=1}^{R} \boldsymbol{s}_r \boxtimes \boldsymbol{b}_r \boxtimes \boldsymbol{a}_r + \boldsymbol{n} \tag{6}$$

where $\boxtimes$ denotes the Kronecker product. Since *measurement* noise vector $\boldsymbol{n}$ is circular white Gaussian and isotropic, *i.e.* $\boldsymbol{\Sigma} = \sigma^2\boldsymbol{I}$, with zero mean and covariance $\sigma^2\boldsymbol{I}$, the log-likelihood then takes the form:

$$\Upsilon(\boldsymbol{\theta}, \boldsymbol{\alpha}, \boldsymbol{\beta}, \boldsymbol{s}) \propto -(\boldsymbol{x}-\boldsymbol{\mu})^{\mathsf{H}}\,\boldsymbol{\Sigma}^{-1}\,(\boldsymbol{x}-\boldsymbol{\mu}) \tag{7}$$

where $\boldsymbol{\mu} = \sum_{r=1}^{R} \boldsymbol{s}_r \boxtimes \boldsymbol{b}_r \boxtimes \boldsymbol{a}_r$ is unknown and constrained by its parameterization. The parameter vector $\boldsymbol{v}$ for $\boldsymbol{\mu}$ is composed of DoAs and factor matrices: $\boldsymbol{v} = [\theta_1, \ldots, \theta_R, \boldsymbol{a}_1, \ldots, \boldsymbol{a}_R, \boldsymbol{s}_1, \ldots, \boldsymbol{s}_R]$. The CRB represents the lower bound on the variance of any unbiased estimator and corresponds to the inverse of the Fisher Information Matrix (FIM). For the derivation of the FIM of the estimation problem in (7), refer to [9] and references therein.

Once factor vectors $\boldsymbol{a}_r, \boldsymbol{b}_r, \boldsymbol{s}_r$ are estimated through a CP decomposition routine, such as Alternating Least Squares (ALS), DoAs can be estimated by:

$$\hat{\theta}_r = \arg\min_{\theta \in \Theta} \left[(\hat{\boldsymbol{b}}_r - \boldsymbol{b}_r(\theta))^{\mathsf{H}} (\hat{\boldsymbol{b}}_r - \boldsymbol{b}_r(\theta)) \right]$$

If $M = 2$, DoAs can also be estimated through the ESPRIT algorithm [13], which is equivalent to the tensor approach in its particular instance for $M = 2$.

Theoretically, this solution can only be approximate, since the minimization has been carried out in two stages. To obtain a more accurate solution, one should maximize the likelihood (7), e.g. by executing an iterative ascent with the suboptimal solution as a starting point. However, this improvement has revealed to be negligible in subsequent computer experiments.

If the acquisition system is composed of $M = 2$ sub-arrays, deduced from each other by a single translation $\boldsymbol{\delta} = \boldsymbol{\delta}_2$, the tensor approach based on model (4) reduces to ESPRIT [13], after inclusion of the unknown sensor gains $g_\ell(\boldsymbol{\theta}_r)$ into $\boldsymbol{A}$:

$$\begin{cases} \boldsymbol{x}_1(t) = \boldsymbol{A}\, \boldsymbol{s}(t) + \boldsymbol{n}_1(t) \\ \boldsymbol{x}_2(t) = \boldsymbol{\Phi}\, \boldsymbol{A}\, \boldsymbol{s}(t) + \boldsymbol{n}_2(t) \end{cases}$$

where $\boldsymbol{\Phi} = \mathrm{Diag}\{e^{-\jmath\omega_0\zeta(\boldsymbol{\theta}_1)}, \cdots, e^{-\jmath\omega_0\zeta(\boldsymbol{\theta}_R)}\}$ is a unitary operator that relates both sub-arrays to each other, and $\zeta(\boldsymbol{\theta}_r) = \boldsymbol{\delta}^{\mathsf{T}} \boldsymbol{d}(\boldsymbol{\theta}_r)/c$. [4]

4 Results for $L = M = 4$

$R = 4$ uncorrelated narrowband sources arriving from $\boldsymbol{\theta} = [25°, 65°, 105°, 345°]$ were simulated with $T = 64$ time samples. Each sub-array is a UCA of radius $\rho_A \approx \lambda/(20\sqrt{2})$ with $L = 4$ sensors, whereas directivity gains are described in Subsection 2.4, with $D = 4$. $M = 4$ sub-arrays with the aforementioned structure are located around a UCA of radius $\rho_B = \lambda/(2\sqrt{2})$ (see Figure 1).

As in [8, 14], SNR is defined as:

$$SNR = 10\log_{10} \frac{\mathbb{E}\left[\boldsymbol{x}^{\mathsf{H}}\boldsymbol{x}\right]}{\mathbb{E}\left[\boldsymbol{n}^{\mathsf{H}}\boldsymbol{n}\right]} = 10\log_{10} \frac{\| \boldsymbol{x} \|_2^2}{LMT\sigma_n^2} \tag{8}$$

and Mean Square Error is defined as $\mathrm{MSE}(\boldsymbol{\theta}) = \frac{1}{\pi^2} \frac{1}{NR} \sum_{n=1}^{N} \sum_{r=1}^{R} (\hat{\theta}_{rn} - \theta_r)^2$.

The approaches compared in Figure 2 refer to tensor DoA estimation: *ALS full* and *CRB full* when sensors are non overlapping and directional, with

[4] If $M = 2$, we also need to fix a half plane ambiguity w.r.t. the translation axis, either thanks to $\boldsymbol{A}$ or thanks to some *a priori* information.

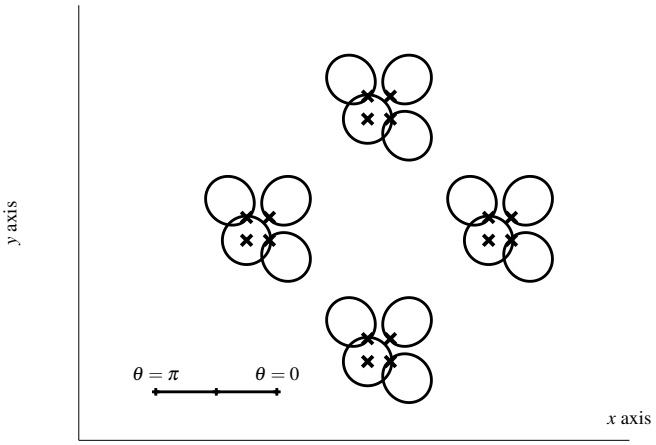

Fig. 1. Acquisition system for $L = M = 4$

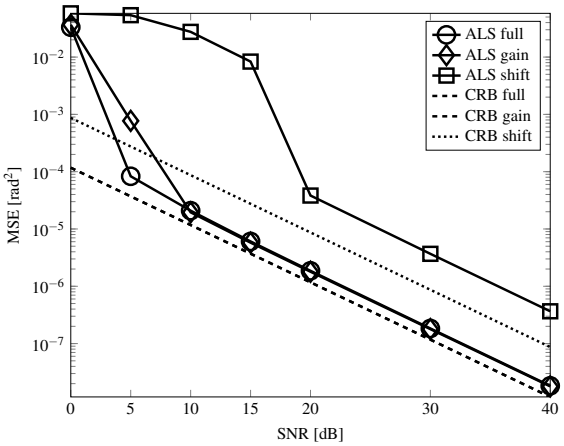

Fig. 2. MSE vs SNR, $D = 4$, $L = M = 4$

$A_{\ell r} = g_\ell(\boldsymbol{\theta}_r)\, e^{-\jmath\omega_0\tau_\ell(\boldsymbol{\theta}_r)}$; *ALS gain* and *CRB gain* when sensors are overlapping and directional, with $A_{\ell r} = g_\ell(\boldsymbol{\theta}_r)$; *ALS shift* and *CRB shift* when sensors are non overlapping and omni-directional, with $A_{\ell r} = e^{-\jmath\omega_0\tau_\ell(\boldsymbol{\theta}_r)}$.

Figure 2 shows that, when sensor positions within a sub-array are not known, the introduction of unknown directional elements improves the estimation. Figure 3 illustrates the dependence of the MSE on sensor directivity D, showing an optimum at $D \approx 4$ (*i.e.* $\gamma \approx 5$) for the present system.

5 Optimization of a Bio-Inspired Microsystem

We consider the case of a small network ($M = 2$) with a few sensors per sub-array. The directivity patterns are chosen according to the anatomy of a fly, that

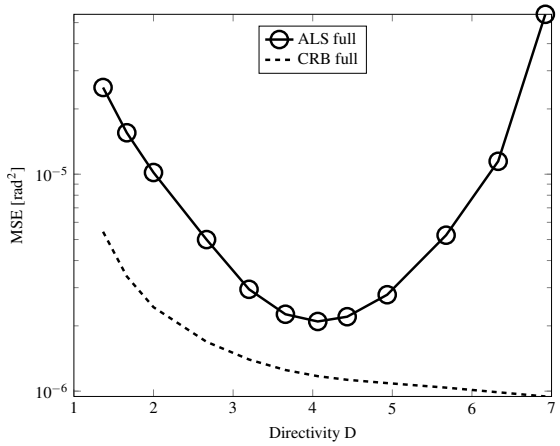

Fig. 3. MSE vs D, $SNR = 20dB$, $L = M = 4$

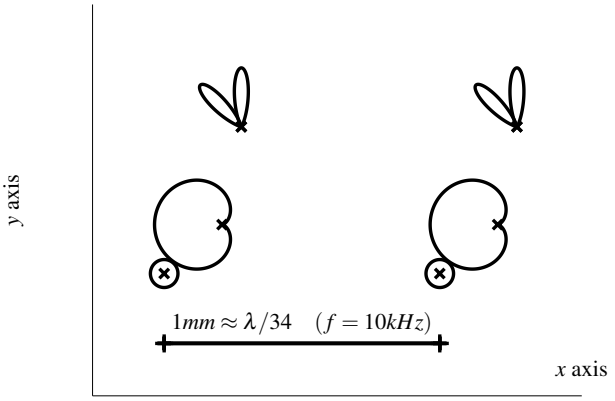

Fig. 4. Bio-inspired sensor network with two sub-arrays: $M = 2$ and $\delta = 1mm$

is known to direct its flight toward other sound emitting insects. We omit the specific physics [11] and focus on the feasibility, in order to reduce the size of the smallest known DoA microsystem [10].

Figure 4 shows the biologically inspired acquisition system: the same group is repeated twice ($M = 2$) through one translation $\delta = 1mm$; impinging sources have identical central frequency $f = 10kHz$ and are simulated from a unit variance random distribution with $T = 64$ time samples. At this working frequency, given the propagation speed of sound through air at 20°, $c = 343.2m/s$, space shift δ corresponds to approximately $\lambda/34$. One sub-array is composed of a reference omnidirectional sensor ($D_1 = 1$ *i.e.* $\gamma_1 = 0$), a main sensor [15] with a cardioid pattern ($D_2 = 2.7$ *i.e.* $\gamma_1 = 2$, $\alpha_2 = 180°$) and two highly directional sensors ($D_3 = D_4 = 17.7$, *i.e.* $\gamma_3 = \gamma_4 = 100$, $\alpha_3 = 90°$ and $\alpha_4 = 135°$) [16].[5]

[5] A cardioid can be defined by 2 parameters: directivity D as described in 2.4 and orientation angle α, that refers to the direction of maximum directivity.

In Figure 5, the results of the proposed algorithm are compared with CRB as a function of SNR, for a given number of impinging sources $R \in \{1, 2\}$. It appears that it is still possible to identify more than one source with a microsystem of the size of the auditory system of a fly, at the cost of a loss of accuracy.

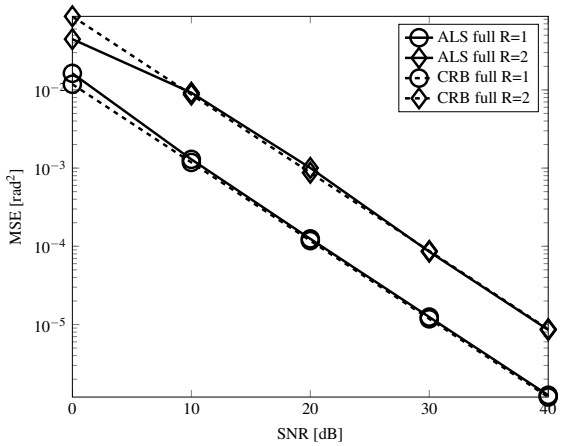

Fig. 5. MSE vs SNR, for $R \in \{1, 2\}$ sources; $\theta \in \{45°, 135°\}$; $\delta = 1mm$, $f = 10kHz$

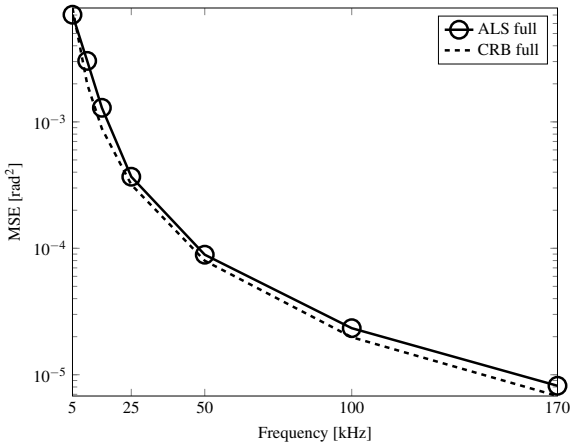

Fig. 6. MSE vs frequency, $R = 2$ sources: $\theta_1 = 45°$, $\theta_2 = 135°$; $\delta = 1mm$, $SNR = 20dB$

In order to face noisy realistic situations, the fly makes use of additional mechanical and neural active solutions, whereas the proposed method may optimize the number of sub-arrays M, space shift δ and working frequency f. Figure 6 shows the MSE as a function of working frequency at $20dB$: performance is optimal for $f = 170kHz$, which corresponds to $\delta \approx \lambda/2$. Equivalently, we could also attain this condition by increasing the space shift δ between the two sub-arrays up to $17mm$, keeping $f = 10kHz$.

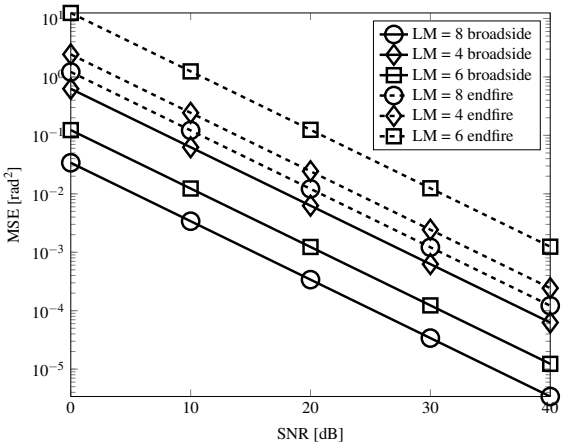

Fig. 7. CRB vs SNR for reduced systems; $R = 2$ sources: broadside: $\theta_1 = 75^\circ$, $\theta_2 = 115^\circ$; endfire: $\theta_1 = 15^\circ$, $\theta_2 = 165^\circ$; $\delta = 1mm$, $f = 10kHz$

Figure 7 illustrates the contribution of particular groups of sensors, by decreasing their number and selecting their directivity patterns, through a customer-driven tradeoff. Three relevant configurations are compared: the first is the 8-sensor configuration of figure 4 ($LM = 8$); the second is formed by the omnidirectional sensor and the big cardioid (total of $LM = 4$ sensors); the third is given by the omnidirectional sensor and the two small and quite directional elements (total of $LM = 6$ sensors).

These configurations are tested for two sets of DoAs: the CRB on the DoAs is plotted for $R = 2$ sources arriving from the broadside or from the endfire of the system. While the CRB of the estimation for the first configuration remains globally the best, the role of the second and the third reduced systems is reversed: the big cardioid is more sensitive to endfire sources, whereas the two quite directional elements are more sensitive to broadside sources. The conclusion is that the two contributions are complementary. Interestingly, only flies which can locate sound emitting distant targets seem to possess a highly sensitive cardioid sensor in each of their two sub-systems.

6 Conclusion

We already knew from [7] that space, time, and translation in space induced exploitable diversities, when omnidirectional sensors are used. This remains true if sensors have known nonzero gain patterns, because they can be compensated. But the question whether sensor gain patterns could induce a diversity was still open. We showed that it can indeed be the case, in particular when sensors are co-located in each sub-array. In that case, there is no space diversity anymore, but tensor approaches can still be applied by using time, pattern and space translation diversities. Our last contribution is the conception of a network of

sensors ($M = 2$, $LM = 4$ to 8) according to the extreme compactness of bio-inspired microsystems. Space translation diversity helps to compensate for non perfectly known directivity patterns of bio-inspired systems.

References

1. T. Rahim and D. Davies, "Effect of directional elements on the directional response of circular antenna arrays," *IEE Proceedings H Microw., Optics and Antennas*, vol. 129, no. 1, pp. 18–22, 1982.
2. M. Chryssomallis, "Smart antennas," *IEEE Antennas and Propag. Mag.*, vol. 42, no. 3, pp. 129–136, 2000.
3. B. R. Jackson, S. Rajan, B. J. Liao, and S. Wang, "Direction of arrival estimation using directive antennas in uniform circular arrays," *IEEE Trans. Antennas Propag.*, vol. 63, no. 2, pp. 736–747, 2015.
4. M. Pesavento and J. Bohme, "Direction of arrival estimation in uniform circular arrays composed of directional elements," in *Proc. IEEE Workshop Sensor Array Multichannel Sig. Process.*, 2002, pp. 503–507.
5. C. Chang, T. Cheng, and H. Lin, "Fast direction finding algorithm for circular array based on directional antenna," in *Intern. Workshop on Microw. Millimeter Wave Circuits Syst. Technol.* IEEE, 2012, pp. 1–4.
6. R. O. Schmidt, "Multiple emitter location and signal parameter estimation," *IEEE Trans. Antennas Propag.*, vol. 34, no. 3, pp. 276–280, Mar. 1986.
7. N. D. Sidiropoulos, R. Bro, and G. B. Giannakis, "Parallel factor analysis in sensor array processing," *IEEE Trans. Signal Process.*, vol. 48, no. 8, pp. 2377–2388, Aug. 2000.
8. S. Sahnoun and P. Comon, "Joint source estimation and localization," *IEEE Trans. Signal Process.*, vol. 63, no. 10, pp. 2485–2495, 2015.
9. F. Raimondi, R. Cabral Farias, O. Michel, and P. Comon, "Wideband multiple diversity tensor array processing," Aug. 2016, working paper or preprint. [Online]. Available: https://hal.archives-ouvertes.fr/hal-01350549
10. X. Zhang, J. Huang, E. Song, H. Liu, B. Li, and X. Yuan, "Design of small MEMS microphone array systems for direction finding of outdoors moving vehicles," *Sensors*, vol. 14, no. 3, pp. 4384–4398, 2014.
11. E. Delevoye, P. Honzik, N. Delorme, and Y. Arthaud, "A new spice-like modeling tool for bio-and electro-acoustic systems including thermoviscous effects," in *Acoustics 2012*, 2012.
12. L. Chiantini and G. Ottaviani, "On generic identifiability of 3-tensors of small rank," *SIAM Journal on Matrix Analysis and Applications*, vol. 33, no. 3, pp. 1018–1037, 2012.
13. R. Roy and T. Kailath, "ESPRIT-estimation of signal parameters via rotational invariance techniques," *IEEE Trans. Acoust. Speech Signal Process.*, vol. 37, no. 7, pp. 984–995, 1989.
14. X. Liu and N. D. Sidiropoulos, "Cramér-Rao lower bounds for low-rank decomposition of multidimensional arrays," *IEEE Trans. Signal Process.*, vol. 49, no. 9, pp. 2074–2086, 2001.
15. N. Tron, H. Stölting, M. Kampschulte, G. Martels, A. Stumpner, and R. Lakes-Harlan, "The Auditory System of the Dipteran Parasitoid Emblemasoma auditrix (Sarcophagidae)," *Journal of Insect Science*, vol. 16, no. 1, p. 90, 2016.
16. J. T. Albert and M. C. Göpfert, "Hearing in Drosophila," *Current opinion in neurobiology*, vol. 34, pp. 79–85, 2015.